2018 IEEE 14th International Conference on Control and Automation (ICCA)
June 12-15, 2018. Anchorage, Alaska, USA

Autonomous Ledge Detection and Landing with Multi-rotor UAV

Swee King Phang[1], Mohamed Redhwan Abdul Hamid[2], Xudong Chen[2], Feng Lin[2]

***Abstract*— As surveillance and reconnaissance utilizing UAVs become more prominent today thanks to the advancement in MEMS sensors and small yet powerful microprocessors, vertical-take-off-and-landing (VTOL) vehicles such as multi-rotor UAVs dominate this area due to its capability of hovering in the air. The endurance, however, is a downside of such operation. In this manuscript, we propose a surveillance solution with multi-rotor UAV by perching at the edge of roof near the target-of-interest, enabling long hour monitoring capability. Challenges on the mechanical design and autonomous ledge detection of the UAV will be addressed and possible solutions will be discussed. Flight experiments were conducted and positive results will be published in this manuscript.**

I. Introduction

Over the years, research on unmanned aerial vehicles (UAVs) has been one of the leading topics in universities and research institutions. With the introduction of multi-rotor UAV in early year 2000, the ease of mechanical design of such UAV has led to multiple research on the control of such UAV, for example in [1], [2]. Then, as the control of multi-rotor system has reached a mature stage, researchers has switched their focuses to vision-based UAV localization methods [3], [4], [5], and towards LiDAR-based localization and mapping on UAV [6], [7], [8].

Besides the fundamental development of the UAVs as described above, many UAV systems were developed to perform specific operations, such as vertical replenishment of goods [9], recovery of UAVs on ships [10], and many more. One particular operation that is useful for surveillance that has not been widely explored by the researcher is the perching of small scale UAV on the edge of building roof. Specifically in Singapore, most of the high-rise building has ledges on their roof, as shown in Fig. 1.

As surveillance and reconnaissance using UAVs becoming more prominent today, vertical-take-off-and-landing (VTOL) vehicles such as multi-rotor UAVs dominate this area due to its capability of hovering in the air [11]. The endurance, however, is the downside of such operation. A typical mutli-rotor UAV can last approximately 20 to 30 minutes while staying stationary in the air, while usually a surveillance job requires much longer period than this. In 2012, DARPA has launched a UAV related challenge called UAVForge, with one of the mission on the surveillance of a remote target area for a duration of 3 hours [12], [13]. It is almost impossible for a multi-rotor UAV to last this long in the air. Instead, the UAV can be commanded to land and perch along the edge of roof of the buildings around the area of interest.

Fig. 1. Typical roof top with ledge of buildings in Singapore

In this manuscript, the development of a small scale multi-rotor UAV for the application of perching at ledges on the roof will be discussed. The area of discussion includes UAV platform modification for secure landing on ledge in Section II, autonomous flight control design for such a UAV in Section III, robust real-time ledge detection with LiDAR sensor in Section IV, and some of the flight trial results with the proposed algorithm in Section V. Finally concluding remarks to be made in the last section.

II. Hardware Platform

This section will discuss and provide the specifications of the UAV chosen for the task of autonomous ledge detection and landing. The decision was based on the the following criteria:

1) A UAV capable to implement our proposed flight controller (i.e., self developed flight control software);
2) A UAV with sufficient load carrying capacity for essential sensors for perching operation to be carried in flight; and
3) Sufficient flight endurance ($>$ 10 minutes) for the whole flight profile.

The custom built multi-rotor platform from the National University of Singapore, codenamed T-Lion, was chosen as the platform for the mentioned task. It had a flight endurance of up to 15 minutes on a single 8000 mAh Lithium polymer (LiPo) battery, a payload carrying capacity of up to 2 kg with a bare 3 kg of fuselage weight.

To enable physical landing on the ledge, a landing device was designed for the specific case of landing on a rectangular

[1]Swee King Phang is with School of Engineering, Taylor's University, 1 Jalan Taylors, 47500 Subang Jaya, Selangor, Malaysia. sweeking.phang@taylors.edu.my

[1]Mohamed Redhwan, Xudong Chen, and Feng Lin are with Temasek Laboratories, National University of Singapore, Singapore {tslmor,tslcx,linfeng}@nus.edu.sg

shaped ledge, as appears in most of the buildings in Singapore. The criteria for the landing device is set as follows:

1) Able to secure the UAV at the ledge;
2) Provides physical allowance for landing in real time dynamic environment to allow reduced control performance due to surrounding disturbances; and
3) Simple and lightweight design.

Further details of UAV hardware and landing mechanism are provided in the following subsections

A. Flight Control Board

As the most essential and flight critical avionic component on any UAV, the custom flight control board has been designed based on the Pixhawk PX4 flight stack and further complemented with reliability and active failsafe in mind. It features 2 separate IMUs, upgraded electronic components, redesigned board ports which prevent loose and inadvertent connections. Flight control software was built and branched out of Pixhawk open source flight control software. It is now include model-based flight controllers which will be discussed in the next section.

B. Laser Range Finder

The sensor to realized autonomous ledge detection is a 2D LiDAR sensor. In our proposed solution, it will be used to accurately determine the height of the UAV relative to the landing point, and the lateral difference between the UAV and the ledge to be perched. A Hokuyo UTM 31-LX provides precise position data at up to 30 m, which is ideal for our algorithm to be working well.

C. Gimbal Controlled Camera System

A camera system is needed to determine the rough position of the ledge, and to align the direction of the ledge to the heading angle of the UAV, as it is important to land in the correct orientation. The focus of this manuscript is on the UAV hardware design and LiDAR ledge detection algorithm, thus the algorithm in vision system will not be discussed here. Nonetheless, the camera system is included in the hardware section for completeness.

An aftermarket 2 axis gimbal system was installed and tuned to enable a camera to be used for the UAVs horizontal positioning. The criteria of the gimbal was simple in that it needed to be able to stabilize the camera in all flight profiles and conditions pointing downwards while being as light a system as possible to maximize flight time.

D. On-board Computer

The Intel NUC is chosen as the on-board processing computer as it houses a powerful i7 processor which can provide data processing, data telemetry to the ground control station and autonomous flight planning for the UAV. The proposed algorithm to detect ledge position and height of the UAV will be implemented and run in this on-board computer in real time. On top of that, a built in Wi-Fi module in the NUC enable operators to send commands to the UAV or to monitor UAV statuses during operation.

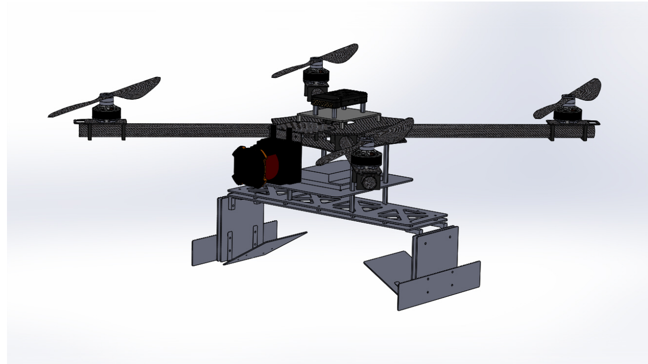

Fig. 2. Perching Mechanism CAD Drawing

Fig. 3. Photo of prototype perching UAV based on T-Lion platform

E. Perching Mechanism Design

In order to securely perch on the building ledge, a perching clamp mechanism is designed at the bottom of the UAV. The clamp mechanism is designed as a compression type clamp with spring steel flat V-springs angled at 60 degrees attached to 3K carbon fiber plates, as shown in Fig. 2. At full compression of the springs, the length between the 2 plates measures 210 mm, which would allow a 50 mm error margin for the UAV control performance. The side plates have a layer of vulcanized foam to provide some impact absorption and grip, while the bottom of the landing plate has 2 layers of high density polyurethane foam for shock and impact absorption. The perching mechanism was designed such that upon landing, should the UAV be offset from the center of the ledge, the UAV would slide into central location by virtue of the angled side plates. The springs would help to clamp onto both sides of the ledge even if the UAV doesn't centre itself perfectly. A modified T-Lion UAV together with its perching clamp mechanism is shown in Fig. 3.

III. Flight Control

In order for autonomous landing on ledge, UAV position control is essential. The UAV control problem is split into two different layers, where the inner-loop controls the attitude of the UAV, and the outer-loop controls the position of the UAV. The overall control flow diagram can be viewed in Fig. 4.

The attitude stabilization layer involves the design of a controller which ensures the UAV roll, pitch and yaw dynamics are robustly stable. Moreover, the position tracking layer involves the design of another controller with lower bandwidth which enables the UAV to track any smooth 3-D trajectory in a responsive and precise way.

The inner-loop controller is implemented in the flight controller board, where an attitude stabilizer is implemented and tuned towards fast closed-loop dynamics with a simple software framework. As large amounts of our work about multi-rotor stability control have been published and documented in [14], [15], the details are omitted in this manuscript.

In contrast, the design of the outer-loop controller is far more critical for this application due to the requirements to land precisely on the ledge, with less than ± 5 cm accuracy is needed. The robust and perfect tracking (RPT) control concept from [16] which was proven to have fast settling time perfectly fits this requirement.

According to [2], the outer dynamics of the quad-rotor UAV is differentially flat. Thus, all its state variables and inputs can be expressed in terms of algebraic functions of flat outputs and their derivatives, i.e.,

$$\sigma = [x, y, z, \psi]^{\mathrm{T}}. \tag{1}$$

For the case of quad-rotor UAV, the first three outputs, x, y, z, are totally independent, as they can be individually controlled. In other words, when designing its outer-loop control law and generating the position references, the UAV can be considered as a mass point with constrained velocity, acceleration and its higher derivatives in the individual axis of the 3-D global frame. In this case, a stand-alone RPT controller based on double (or triple with integral action) integrator model in each axis can be designed to track the corresponding reference in that axis. In our application, to ensure a good tracking performance, we include an error integral to ensure zero steady-state error. This requires an augmented system to be formulated as

$$\begin{cases} \dot{\boldsymbol{x}}_{\text{aug}} = \begin{bmatrix} 0 & -1 & 0 & 0 & 1 & 0 \\ 0 & 0 & 1 & 0 & 0 & 0 \\ 0 & 0 & 0 & 1 & 0 & 0 \\ 0 & 0 & 0 & 0 & 0 & 0 \\ 0 & 0 & 0 & 0 & 0 & 1 \\ 0 & 0 & 0 & 0 & 0 & 0 \end{bmatrix} \boldsymbol{x}_{\text{aug}} + \begin{bmatrix} 0 \\ 0 \\ 0 \\ 0 \\ 0 \\ 1 \end{bmatrix} u_{\text{aug}} \\ \boldsymbol{y}_{\text{aug}} = \boldsymbol{x}_{\text{aug}} \\ h_{\text{aug}} = \begin{bmatrix} 1 & 0 & 0 & 0 & 0 & 0 \end{bmatrix} \boldsymbol{x}_{\text{aug}} \end{cases}, \tag{2}$$

where $\boldsymbol{x}_{\text{aug}} = \begin{bmatrix} \int(\mathbf{p}_{\text{e}}) & \mathbf{p}_{\text{r}} & \mathbf{v}_{\text{r}} & \mathbf{a}_{\text{r}} & \mathbf{p} & \mathbf{v} \end{bmatrix}^{\mathrm{T}}$, $\mathbf{p}_{\text{r}}$, $\mathbf{v}_{\text{r}}$, $\mathbf{a}_{\text{r}}$ are the position, velocity and acceleration references in the controlled axis, $\mathbf{p}$, $\mathbf{v}$ are the actual position and velocity and $\mathbf{p}_{\text{e}} = \mathbf{p}_{\text{r}} - \mathbf{p}$ is the tracking error of the position. Following the procedures in [17], a linear feedback control law of the following form can be acquired as:

$$u_{\text{aug}} = F_{\text{aug}} \boldsymbol{x}_{\text{aug}}, \tag{3}$$

where

$$F_{\text{aug}} = \begin{bmatrix} \frac{k_i \omega_n^2}{\varepsilon^3} & \frac{\omega_n^2 + 2\zeta\omega_n k_i}{\varepsilon^2} & \frac{2\zeta\omega_n + k_i}{\varepsilon} & 1 & -\frac{\omega_n^2 + 2\zeta\omega_n k_i}{\varepsilon^2} & -\frac{2\zeta\omega_n + k_i}{\varepsilon} \end{bmatrix}.$$

Here, ε is a design parameter to adjust the settling time of the closed-loop system. ω_n, ζ, k_i are the parameters that determine the desired pole locations of the infinite zero structure of (2) through

$$p_i(s) = (s + k_i)(s^2 + 2\zeta\omega_n s + \omega_n^2). \tag{4}$$

Theoretically, when the design parameter ε is small enough, the RPT controller can give arbitrarily fast responses. Nevertheless, realistically it is safer to limit the bandwidth of the outer loop to be much smaller than that of the inner-loop dynamics, because of the constraints of the UAV physical dynamics and its inner-loop bandwidth.

IV. Ledge Position Detection

For autonomous perching on building ledge, using GPS measurement for position estimation alone will introduce large estimation error due to the accuracy of the GPS measurement. On the other hand, the relative position between the ledge and the UAV must be estimated accurately, within a ± 5 cm error as determined by our mechanical design of the UAV shown in previous sections, for successful perching on the ledge.

There are total of 4 variables to be estimated with proximity sensors, i.e., x, y, z-positions and heading angle ψ. Out of these 4 variables to be estimated, the y, z-positions, and the heading angle ψ is especially important for the perfect perching. As shown in Fig. 5, as the ledge is assumed to have constant width (in y-direction) and long-enough (in x-direction) for small estimation error along the ledge, the requirement on y-direction estimation is much higher than in x-direction. On the other hand, in Fig. 6, the heading difference between the UAV and the ledge direction is also important as the perching mechanism on the UAV only works in one direction.

In this research work, a downward looking camera was deployed for visual odometry to estimate the position of the UAV without relying on GPS signals. Besides the camera, a 2D LiDAR sensor was installed to obtain height information and point cloud for the perching site. Heading angle difference algorithm was implemented based on camera images, and it will be discussed in another document together with the visual odometry algorithm utilized by the UAV. In this paper, a detail implementation of z-direction and y-direction estimation using a single 2D LiDAR sensor will be discussed.

A. Split-and-Merge Algorithm

LiDAR scan of yz-plane on the UAV body axes will be obtained at 20 Hz. With each of these scans towards the ground direction (positive z-direction), a 90 degree downwards field-of-view worth of data is collected. There are a total of 361 data points with integer values. Each of these

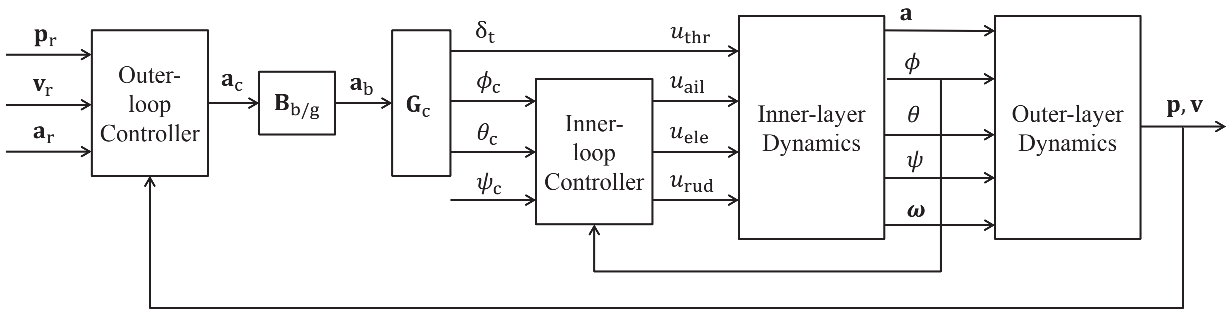

Fig. 4. Dual-loop control structure of the quadrotor

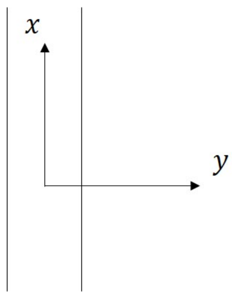

Fig. 5. x, y-position of UAV on ledge parallel to UAV

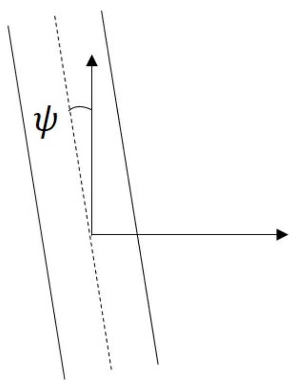

Fig. 6. ψ heading angle difference between UAV and ledge

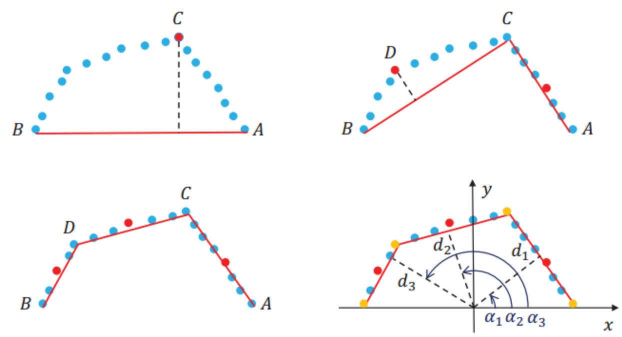

Fig. 7. Steps on *split-and-merge* algorithm

values represents the measured distances in millimeter from its starting point on the right to the ending point on the left, covering a total of 90° angle. These data can be seen as polar coordinates since each distance is associated with its own angle direction. To convert the raw measurement date from polar coordinates (r_i, θ_i) to Cartesian coordinates (x_i, y_i), the following transformation can be applied

$$x_i = r_i \cos\theta_i, \tag{5}$$
$$y_i = r_i \sin\theta_i, \tag{6}$$

where $i \in \{1, 2, 3, ..., 361\}$ is the index of the laser scanner measurements. This array of 2D points is then grouped into clusters of points belonging to individual line segments by the *split-and-merge* algorithm. The main steps of the *split-and-merge* algorithm is summarized as follows with Fig. 7 giving a graphical illustration. More detailed implementation of *split-and-merge* algorithm on UAV is documented in [5].

1) The first point A is connected to the last point B by a straight line.
2) A point C with the highest perpendicular distance to the line AB is identified.
3) If this point C is within a threshold, then a cluster is created containing points in between A and B.
4) Else, the input points will be split into two subgroups, A-C and C-B. For each group, the *split-and-merge* algorithm will be applied recursively.

With the clusters of points created by the above-mentioned algorithm, a least-square line fitting algorithm is applied to all points within each cluster to obtain individual lines. In this case, each line is represented by two parameters–the line's normal direction α_k and its perpendicular distance to the center of laser scanner d_k.

Next, lines with dissimilar gradient as the ground plane are filtered out. Since the obtained lines are expressed in the laser scanner frame, their directions α_k should be compensated by the UAV roll angle ϕ and then compared to the normal line of the ground plane at $\pi/2$. Hence

$$\Delta\alpha_k = \alpha_k - \phi - \pi/2. \tag{7}$$

The corresponding line is filtered out if the value of $\Delta\alpha_k$ is greater than a threshold of 10 degrees. The remaining lines are sorted by their perpendicular distances to the laser scanner and the furthest ones are kept. Among these lines, the longest one is chosen to be the true ground, while the

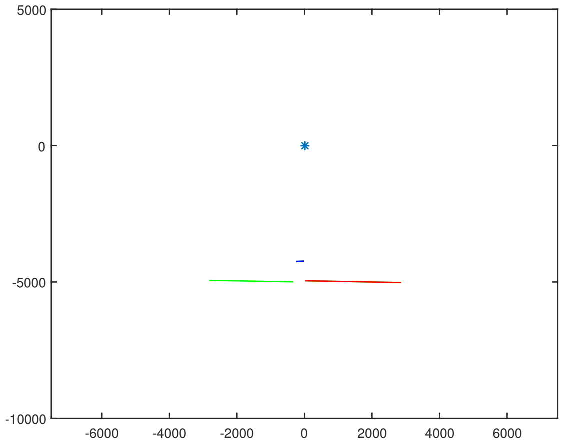

Fig. 8. Results on *split-and-merge* algorithm on actual building ledge

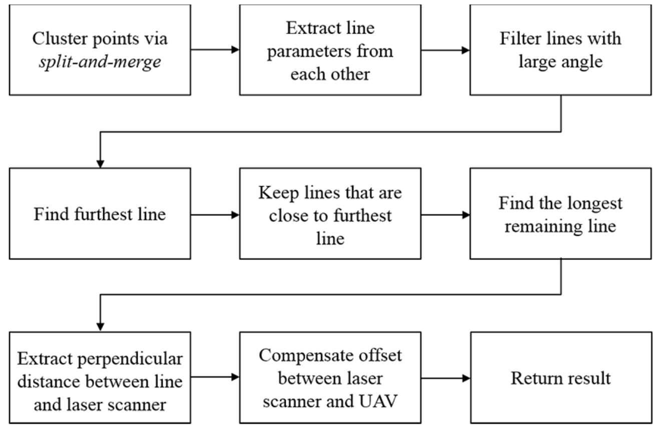

Fig. 9. Steps to compute height and ledge position via 2D LiDAR sensor

parallel line closest to the UAV is assumed to be the ledge cross-section. A snapshot of the result from *split-and-merge* algorithm is shown in Fig. 8, where the asterisk (*) is the UAV position, the three straight lines parallel to the ground are the detected and filtered lines. Out of these 3 straight lines, the red one is chosen to be the truth ground as it has the longest distance, where the blue line is assumed to be the ledge cross-section. The height and ledge point detection algorithm has proven to have at least 95% accuracy from more than 5 flight trials conducted.

With the accurate detection of ground plane and ledge cross-section, the flying height of the UAV and the y-direction relative distance between the UAV and the ledge can be calculated easily. The perpendicular distance of the red line to the laser scanner center is indeed the flying height of the UAV. It is then compensated with the UAV pitch angle θ and the offset between the laser scanner and the UAV center of gravity (CG), Δh, and thus the final height estimation to be

$$h = r\cos\theta - \Delta h. \tag{8}$$

Fig. 9 shows the flow chart of the LiDAR based height and ledge detection algorithm. Using this method, accurate height measurement and ledge position can be obtained as long as the laser scanner projects a portion of its laser beams onto the true ground together with the building ledge. Therefore, it still works for the case when the UAV flies over protruding objects on the ground, such as obstacles along the building wall (ledge).

V. Flight Trials

The algorithms and controller mentioned in the previous sections are implemented in T-Lion. A proof-of-concept flight trial was carried out in the presence of VICON system, where the position and heading angle of the UAV are measured and given by the external motion tracking system as ground truth to compare with the estimation from our proposed algorithm. As the experiment was done indoor,

Fig. 10. Left: Actual roof ledge; Right: Mock up ledge

a mock up ledge resembling the actual roof ledge was constructed as in Fig. 10. In this experiment, the T-Lion was commanded to take-off, fly towards a mock-up ledge in the setup, and then proceed to descend and perch on the ledge. A snapshot of the T-Lion in action is shown in Fig. 11 in the VICON-controlled environment.

In this flight experiment, the position data obtained from VICON motion tracking system is compared to the estimation results using the mentioned LiDAR height and ledge point detection algorithm. Fig. 12 and Fig. 13 shows a ground truth comparison of the position estimated by our proposed algorithm with the measurement obtained from the VICON system directly (as ground truth). It is noted that the estimated measurement with our proposed algorithm managed to maintain 100% of positive detection rate as long as the ledge is within the LiDAR sensor's field-of-view. Table I shows the largest error of both the height and ledge point detection algorithm.

VI. Conclusions

In this manuscript, a detail implementation methodology of a multi-rotor UAV perching system is presented. The proposed ledge detection and localization method with LiDAR sensor is discussed and its result is supported by ground truth

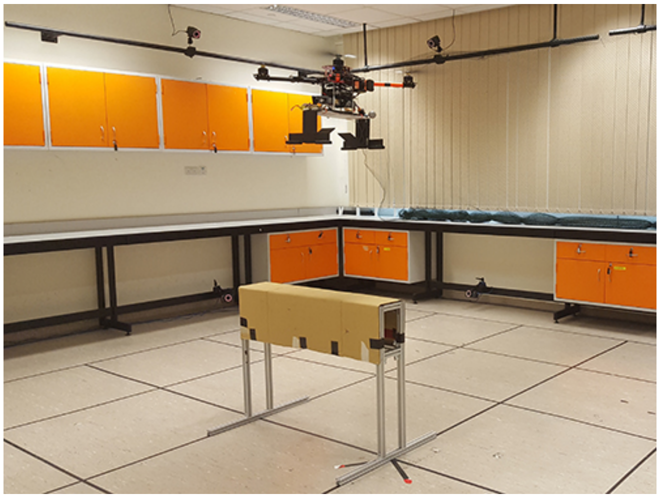

Fig. 11. T-Lion before landing on mock-up ledge in VICON environment

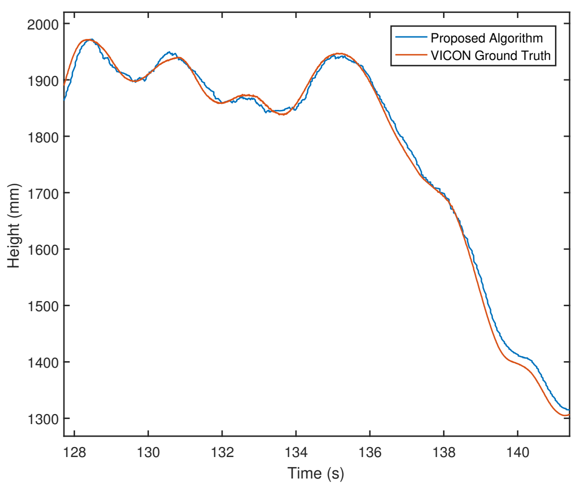

Fig. 12. Height of UAV in VICON environment compared to the estimated results from the proposed algorithm

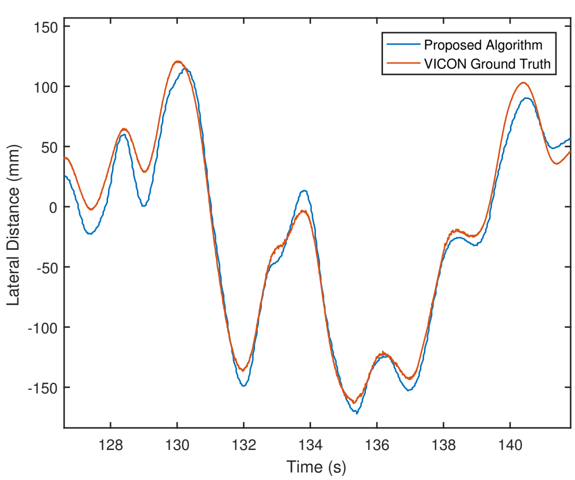

Fig. 13. Lateral position of UAV in VICON environment compared to the estimated results from the proposed algorithm

TABLE I
ACCURACY OF PROPOSED ALGORITHMS

	Largest Error
Height	24.0 mm
Lateral Position	19.9 mm

data obtained from actual flight trials. The perching clamp mechanism is also proven to work well with the mock up ledge, which is similar to a majority of the building ledges in Singapore. With this mechanical consideration in design, the system should work well even in the presence of light environmental disturbances.

REFERENCES

[1] A. Imam and R. Bicker, "Design and construction of a small-scale rotorcraft uav system," *International Journal of Engineering Science and Innovative Technology (IJESIT)*, vol. 2, 2014.

[2] D. Mellinger and V. Kumar, "Minimum snap trajectory generation and control for quadrotors," in *Robotics and Automation (ICRA), 2011 IEEE International Conference on*, pp. 2520–2525, IEEE, 2011.

[3] B. Herissé, T. Hamel, R. Mahony, and F.-X. Russotto, "Landing a vtol unmanned aerial vehicle on a moving platform using optical flow," *IEEE Transactions on robotics*, vol. 28, no. 1, pp. 77–89, 2012.

[4] S. Lange, N. Sunderhauf, and P. Protzel, "A vision based onboard approach for landing and position control of an autonomous multirotor uav in gps-denied environments," in *Advanced Robotics, 2009. ICAR 2009. International Conference on*, pp. 1–6, IEEE, 2009.

[5] X. Chen, S. K. Phang, M. Shan, and B. M. Chen, "System integration of a vision-guided uav for autonomous landing on moving platform," in *Control and Automation (ICCA), 2016 12th IEEE International Conference on*, pp. 761–766, IEEE, 2016.

[6] L. Kaul, R. Zlot, and M. Bosse, "Continuous-time three-dimensional mapping for micro aerial vehicles with a passively actuated rotating laser scanner," *Journal of Field Robotics*, vol. 33, no. 1, pp. 103–132, 2016.

[7] F. Wang, J. Cui, S. K. Phang, B. M. Chen, and T. H. Lee, "A mono-camera and scanning laser range finder based uav indoor navigation system," in *Unmanned Aircraft Systems (ICUAS), 2013 International Conference on*, pp. 694–701, IEEE, 2013.

[8] M. Bosse, R. Zlot, and P. Flick, "Zebedee: Design of a spring-mounted 3-d range sensor with application to mobile mapping," *IEEE Transactions on Robotics*, vol. 28, no. 5, pp. 1104–1119, 2012.

[9] S. Zhao, Z. Hu, M. Yin, K. Z. Ang, P. Liu, F. Wang, X. Dong, F. Lin, B. M. Chen, and T. H. Lee, "A robust real-time vision system for autonomous cargo transfer by an unmanned helicopter," *IEEE Transactions on Industrial Electronics*, vol. 62, no. 2, pp. 1210–1219, 2015.

[10] M. Garratt, H. Pota, A. Lambert, S. Eckersley-Maslin, and C. Farabet, "Visual tracking and lidar relative positioning for automated launch and recovery of an unmanned rotorcraft from ships at sea," *Naval Engineers Journal*, vol. 121, no. 2, pp. 99–110, 2009.

[11] F. Kendoul, "Survey of advances in guidance, navigation, and control of unmanned rotorcraft systems," *Journal of Field Robotics*, vol. 29, no. 2, pp. 315–378, 2012.

[12] K. S. Kumar and A. M. Rasheed, "Development of rotary wing mini uas for civilian applications," *Unmanned Systems*, vol. 1, no. 02, pp. 247–258, 2013.

[13] F. Lin, K. Z. Ang, F. Wang, B. M. Chen, T. H. Lee, B. Yang, M. Dong, X. Dong, J. Cui, S. K. Phang, *et al.*, "Development of an unmanned coaxial rotorcraft for the darpa uavforge challenge," *Unmanned Systems*, vol. 1, no. 02, pp. 211–245, 2013.

[14] S. K. Phang, S. Lai, F. Wang, M. Lan, and B. M. Chen, "Systems design and implementation with jerk-optimized trajectory generation for uav calligraphy," *Mechatronics*, vol. 30, pp. 65–75, 2015.

[15] S. K. Phang, K. Li, K. H. Yu, B. M. Chen, and T. H. Lee, "Systematic design and implementation of a micro unmanned quadrotor system," *Unmanned Systems*, vol. 2, no. 02, pp. 121–141, 2014.

[16] B. M. Chen, T. H. Lee, and V. Venkataramanan, *Hard disk drive servo systems*. Springer Berlin, 2002.

[17] B. M. Chen, *Robust and H_∞ Control*. Springer, 2000.